

Article

Enhanced Performances of Quantum Dot Light-Emitting Diodes with An Organic–Inorganic Hybrid Hole Injection Layer

Ling Chen ^{1,*}, Donghuai Jiang ¹, Wenjing Du ¹, Jifang Shang ¹, Dongdong Li ^{2,*} and Shaohui Liu ^{1,*}

¹ College of Materials Engineering, Henan Key Laboratory of Electronic Ceramic Materials and Application, Henan University of Engineering, Zhengzhou 451191, China.

² Huaibei Yeelight Technology Co., Ltd., Huaibei 235000, China

* Correspondence: cling555@163.com (L.C.); lidongdong@yeelight.com (D.L.); qqliushaohui@163.com (S.L.)

Abstract: PEDOT:PSS (polyethylene dioxythiophene:polystyrenesulfonate) is a commonly used hole injection layer (HIL) in optoelectronic devices due to its high conductive properties and work function. However, the acidic and hygroscopic nature of PEDOT:PSS can be problematic for device stability over time. To address this issue, in this study, we have demonstrated the potential of an organic-inorganic hybrid HIL, by incorporating solution-processed WO_x nanoparticles (WO_x NPs) into the PEDOT:PSS mixture. This hybrid solution was found to have a superior hole transport ability and low Ohmic contact resistance, contributing to higher brightness (~62 000 cd m⁻²) and current efficiency (13.1 cd A⁻¹) in the manufactured quantum-dot based light-emitting diodes (QLEDs). In addition, the resulting devices achieved a relative operational lifetime of 7,071 hours, or approximately twice that of traditional QLEDs with PEDOT:PSS HILs. The proposed method is an uncomplicated, reliable and low-cost way to achieve long operational lifetimes without sacrificing efficiency in optoelectronic devices.

Keywords: WO_x nanoparticle doped PEDOT:PSS; hole injection layer; quantum dot; light-emitting diode

1. Introduction

Quantum Dot light-emitting diodes (QLEDs), are becoming increasingly popular as a potential choice for future light-emitting applications. This is mainly due to their unique features such as tunable colors, high color purity, low cost solution processability and inherent photophysical stability [1-5]. The first successful demonstration of QLEDs was conducted by A.P. Alivisatos [6], and since then, the external quantum efficiency (EQE) has improved significantly, reaching values above 30%. This has been made possible by the advancement of process technology and the accumulation of knowledge on materials and device architectures [7-9]. The most advanced QLED structures currently available, incorporate a multi-layer design, which sandwiches the QD emitting layer between an inorganic electron transport layer and an organic hole injection/transport bi-layer (HIL/HTL). The HIL usually consists of poly(3,4-ethylenedioxythiophene): polystyrene sulfonate (PEDOT: PSS) due to its high work function, low-temperature solution processability, high transparency, and conductivity [1,4,7-9]. However, despite achieving high efficiency, the moisture- and acid-sensitive nature of the PEDOT:PSS HIL often leads to device degradation, thereby limiting performance and operational stability [10,11].

To address the issues with PEDOT: PSS, solution-processed transition metal oxides such as NiO, MoO₃, WO_x, CuO, and V₂O₅ have been explored as alternative HILs in QLEDs due to their high stability to heat, hydrogen, and oxygen [12-16]. While these metal oxides have demonstrated improved device stability, there are still challenges to overcome, such as energy level mismatch and poor crystallinity [17-19], which can limit the luminescent performance of devices.

To address these challenges, bi-layer PEDOT:PSS [17,18,20] and transition-metal oxide doped PEDOT:PSS [21-23] have been successfully adopted in the field of various optoelectronics. In fact, organic-inorganic hybrid HILs have shown promise for improving QLED stability and performance. In our previous work [18], we have demonstrated that a WO₃/PEDOT:PSS bilayer HIL can improve lifetime without sacrificing efficiency. Shin et. al have also reported success using PEDOT:PSS:V₂O₅ films as the HIL prepared by a sol-gel method, resulting in all solution-processed QLEDs with maximum luminance and current efficiency values of 36 198 cd m⁻² and 13.9 cd A⁻¹, respectively [23]. Therefore, the development of new organic-inorganic hybrid materials is a promising method for advancing the field of QLEDs.

In this study, we have demonstrated that a high-quality organic-inorganic hybrid HIL, possessing superior hole transport ability and low Ohmic contact resistance, can be easily formulated by mixing a precise amount of solution-processed WO_x nanoparticles (WO_x NPs) into PEDOT:PSS. By incorporating WO_x NPs, we were able to achieve full solution-processed QLEDs with significantly improved luminance and current efficiency, which also exhibited a longer device lifetime. Our findings highlight that using the organic-inorganic hybrid HIL in QLEDs is a cost-effective and reliable method, with uncomplicated experimental procedures, to achieve longer operational lifetime without compromising efficiency.

2. Materials and Methods

Synthesis of green alloy structure CdSe@ZnS, ZnO and WO_x NPs. As per our previous works [24], the green CdSe@ZnS QDs were synthesized. To prepare WO_x NPs, the hydration method reported previously [25] was followed. In this method, hydrochloric acid solution was slowly added to aqueous ammonium metatungstate hydrate solution with stirring under a constant rate until the pH of the mixed solution was in between 1 and 1.25 at room temperature. Subsequently, the solution was heated and stirred for 1 hour. Prior to use, the WO_x solution was filtered using a 0.45 mm membrane filter. The colloidal ZnO NPs were synthesized by following a reported method [1]. The as-synthesized ZnO NPs were washed twice with heptane and the particles were finally dispersed in ethanol for our experiment (approx. 30 mg mL⁻¹).

Fabrication of QLED Device. Firstly, ITO-coated glass substrates with a sheet resistance of approximately 15 Ω sq⁻¹ were sequentially cleaned in ultrasonic baths containing detergent, de-ionized water, acetone, and isopropanol for 15 minutes each. The substrates were then exposed to an ultraviolet ozone ambient for 15 minutes. After this cleaning procedure, PEDOT: PSS solutions or WO_x: PEDOT: PSS solutions with different blend ratios were spin-coated onto the substrates at 5000 rpm and baked at 150 °C for 15 minutes. The substrates were then transferred to a N₂-filled glovebox for the deposition of TFB, QDs, and ZnO NPs layers. TFB was dissolved in chlorobenzene with a concentration of 8 mg mL⁻¹ and spin-coated at 3000 rpm and annealed at 150 °C for 30 minutes. The green QDs were dispersed in chloroform with a concentration of 15 mg mL⁻¹ and then spin-coated at 3000 rpm for 60 seconds. Next, the ZnO NPs were deposited at a speed of 1500 rpm as electron transport layers (ETLs). The multilayer samples were then loaded into a high-vacuum deposition chamber, where the Al cathode (100 nm) was thermally deposited at a pressure of ≤1 × 10⁻⁶ mbar. Finally, the QLED devices were encapsulated using ultraviolet-curable resin and cover glasses.

Characterization Transmission Electron Microscope (TEM) images of QDs and WO_x NPs were recorded by using a JEOL JEM-2100 electron microscope. The absorption spectra of both the QDs and WO_x solutions was measured using an UV-vis spectrometer (Lambda 950, PerkinElmer, USA). The PL spectra were collected using a spectrofluorometer (JY HORIBA FluoroLog-3). A scanning electron microscope (SEM) (Nova Nano SEM 450) and atomic force microscopy (AFM) (Dimension Icon) was used to obtain the surface topography images. The current density–luminance–voltage (J-V-L) characteristics and electroluminescence spectra of the QLEDs were measured under ambient conditions using a Keithley 2400 sourcemeter and a PhotoResearch spec-trometer PR-735.

3. Results and Discussions

3.1. Characterization of WO_x NPs

The morphology and size of the synthesized WO_x NPs were studied using TEM. As shown in Figure 1(a), the WO_x NPs are spherical particles with an average diameter of approximately 20 nm. However, the WO_x NPs tend to aggregate due to interactions between them, highlighting the need for the introduction of suitable ligands to improve their dispersion in future. The absorption spectrum in Figure 1(b) indicates that the WO_x solution retains a high transmission across the entire visible spectrum. This is crucial for our thin film QLED designs, which will be discussed later in this article. Moreover, the band gap energy (E_g) of WO_x NPs can be determined by the relation $\alpha h\nu = (h\nu - E_g)^m$, where $m = 1/2$ for direct bandgap semiconductors [26]. The linear section of the curve (in Figure 1(b), inset) can be extrapolated to the zero absorption coefficient, allowing the estimation of E_g as 3.8 eV. The XRD patterns of the as-prepared and annealed WO_x films are shown in Figure 1(c). The as-prepared WO_x film is amorphous, but the film becomes crystalline at 300 °C, with various stoichiometric states forming.

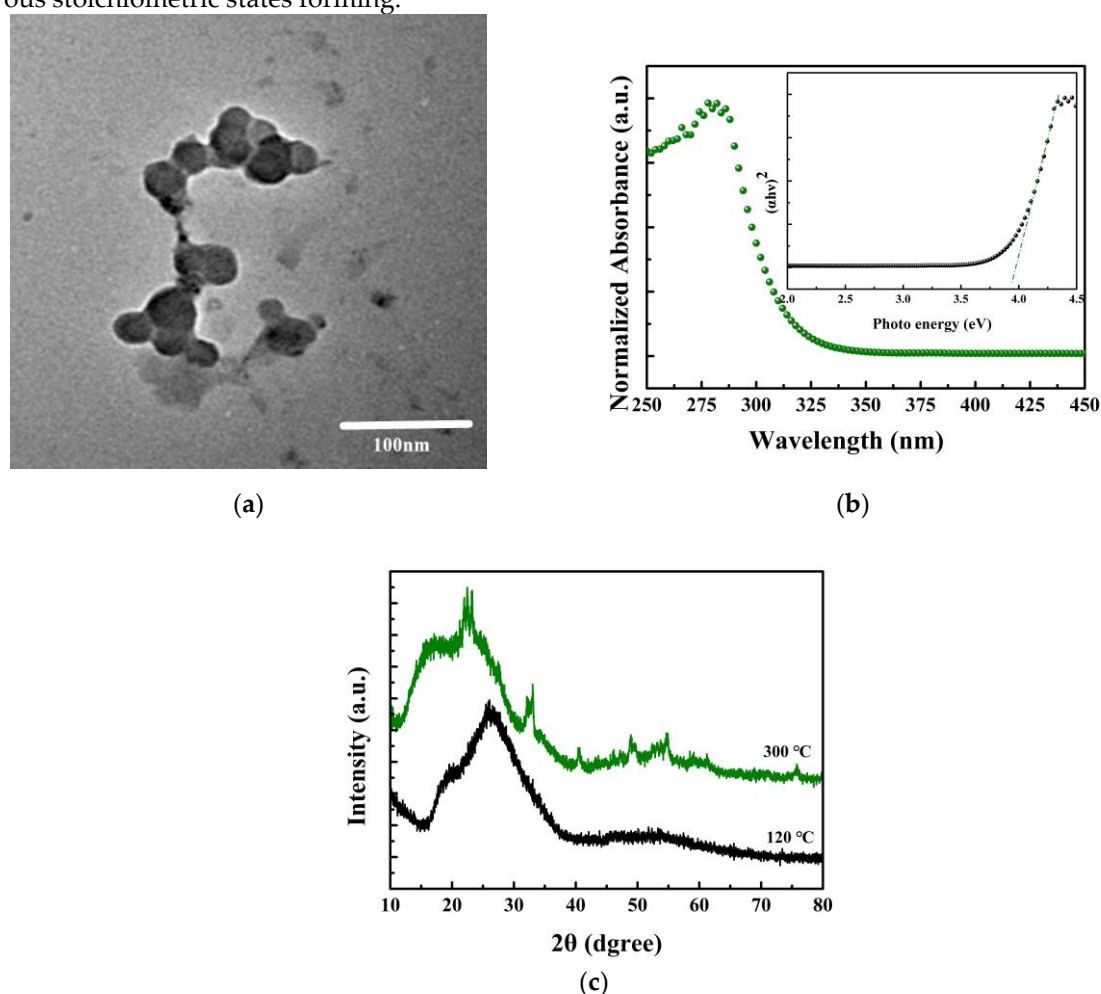


Figure 1. (a) The TEM micrographs of the as prepared WO_x NPs; (b) Ultraviolet-visible absorption spectrum of WO_x film. The inset shows a plot of absorption coefficient vs. photon energy for the determination of the WO_x optical band gap; (c) XRD patterns of WO_x films (annealed at 120 °C and 300 °C, respectively).

The composition of WO_x films was analyzed using X-ray photoelectron spectroscopy (XPS) spectra, which are illustrated in Figure 2. The O 1s peak was found to be at 530.1 eV. The XPS spectrum of the W 4f core level, as shown in Figure 2(b), revealed peaks at 33.2 eV (W 4f_{7/2}) and 35.4 eV (W 4f_{5/2}) which can be attributed to the high oxidation state of W in WO_x. Additionally, a broad

peak of 5p_{3/2} was observed at approximately 39.3 eV. As per previous literature [27, 28], these peak positions and shapes have been designated to represent the WO_x compound in W⁶⁺.

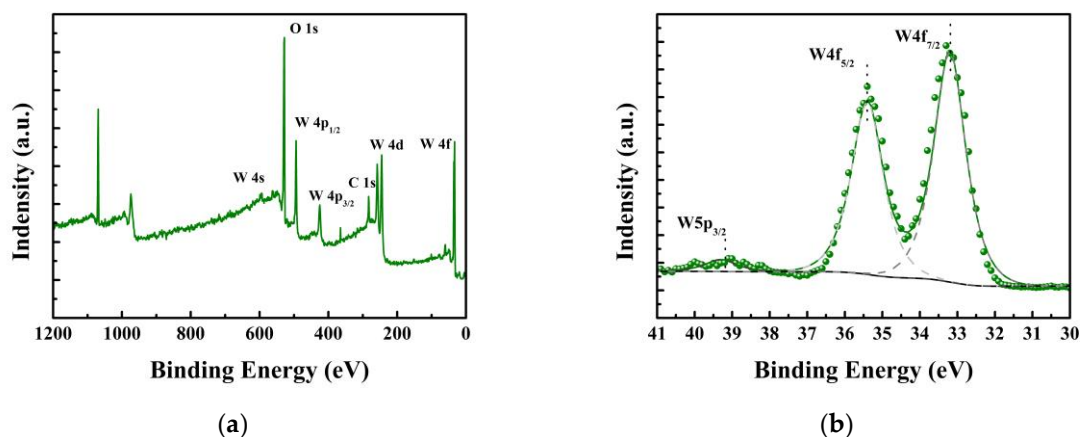


Figure 2. (a) Wide-scan XPS spectrum of the WO_x films; (b) W 4f XPS spectrum of the WO_x and its peak fitting.

3.2. QLED performance

The green alloy structure CdSe@ZnS QDs were selected as the emitting layer, as they possess a spherical shape with an average diameter of approximately 10 nm (as illustrated in Figure 3(a)). The UV-vis and PL characteristics of the CdSe@ZnS QDs were examined, with the PL peak observed at 519 nm, without any surface defect-related emissions (as demonstrated in Figure 3(b)). Photographs of the excited QDs in methylbenzene were included in the insets. The difference in wavelengths between the absorption and PL spectra band maxima is primarily caused by the Stokes shift [29].

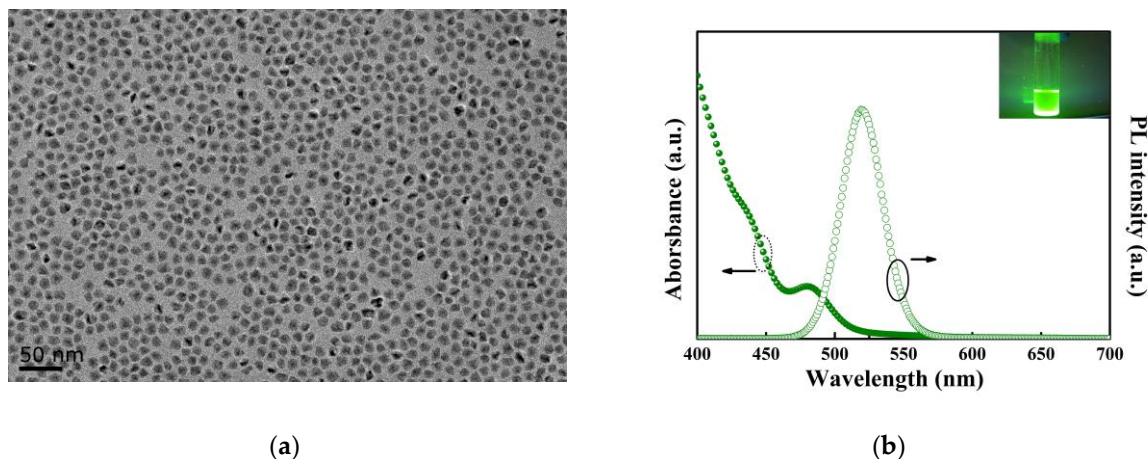


Figure 3. (a) TEM image of CdSe@ZnS QDs; (b) PL and absorption spectra of the QDs in methylbenzene. (The inset shows the image of the QDs dispersed in methylbenzene)

In this study, a thin film was formed by spin coating and annealing a mixture of PE-DOT:PSS and tungsten oxide in a certain proportion, which acted as a HIL for QLEDs, as illustrated in Figure 4(a). The control QLED device had a multilayer architecture (Figure 4(b)) consisting of an ITO anode, a PEDOT:PSS or WO_x:PEDOT:PSS HIL, a TFB hole HTL, a green QD EML, ZnO nanoparticles ETL, and Al cathode. Based on the energy level diagram (Figure 4(c)), the injection of electrons into the QD emissive layer in QLEDs is slightly easier compared to the injection of holes due to a smaller energy barrier between ZnO NPs and QDs. The addition of the WO_x layer has further strengthened hole injection in green CdSe@ZnS QLEDs, resulting in a shift of the major recombination center towards the QDs/ZnO interface and a significant enhancement of the recombination rate [30]. The WO_x layer has effectively acted as an electric dipole layer, with electrons diffusing from PE-

DOT:PSS and TFB to the deep-lying conduction band of WO_x (~6.5 eV) and leaving holes in PEDOT:PSS and TFB.

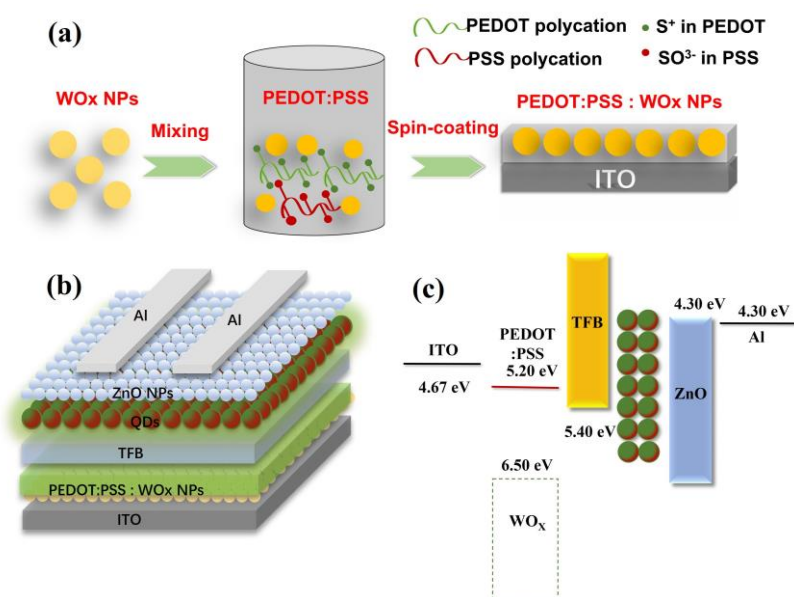
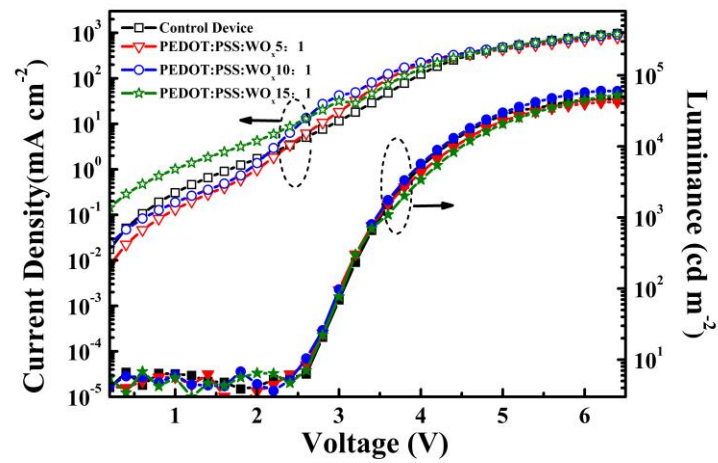


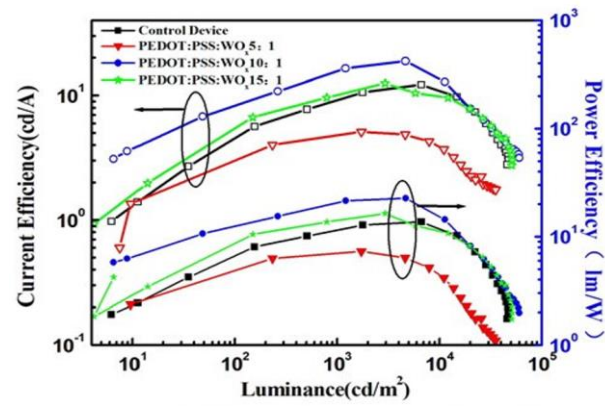
Figure 4. (a) Schematic diagram of the preparation and formation process of WO_x: PEDOT:PSS films; (b) The structure of QLED and the functional layer materials used in this work; (c) Schematic illustration of the energy level diagram.

The J–L–V characteristics and current efficiency–power efficiency with luminance (CE–PE–L) of the QLEDs are presented in Figure 5(a,b), with the volume ratio of PEDOT:PSS and WO_x ranging from 5:1 to 15:1 to determine the optimal ratio. Table 1 summarizes the performance parameters of QLEDs using mixtures of PEDOT:PSS and WO_x as HTLs. The maximum brightness of the standard device is 46000 cd m⁻², but the optimized device with a 10:1 ratio of PEDOT:PSS: WO_x HIL achieves a maximum brightness of 62000 cd m⁻², a 34.7% increase. Figure 5(a) shows that both the devices have a low turn-on voltage of ~2.7 V, indicating efficient carrier injection into the QD layer. The enhanced hole injection can improve charge balance and ultimately enhance the device's efficiency, as demonstrated by the CE and PE curves in Figure 5(b). For instance, the standard device achieved the maximum CE of 9.8 cd A⁻¹ at a voltage of 3.8 V. In contrast, the device incorporating 10:1 PEDOT:PSS:WO_x HIL achieved the same value of CE with just 3.5 V and exhibited a maximum CE increase of approximately 33.7%, reaching 13.1 cd A⁻¹. Additionally, while standard QLEDs exhibited the maximum PE of 6.5 lm W⁻¹, devices with 10:1 PEDOT:PSS:WO_x HIL achieved a maximum PE of 8.9 lm W⁻¹, indicating a 36.9% increase compared to pure PEDOT:PSS. This improved performance is attributed to the introduction of WO_x, which increases carrier mobility and the probability of electron-hole radiative efficiency within the QD layers.

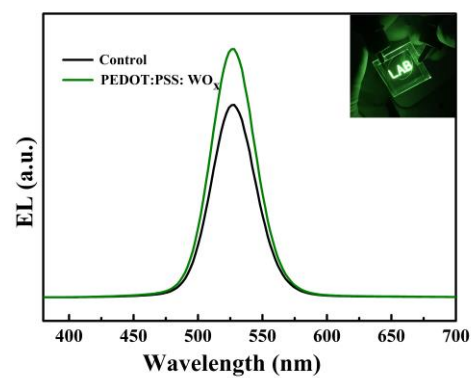
Figure 5(c) illustrates the EL spectra of the standard and optimal QLEDs at 3.5V. The spectra reveal a Gaussian-shaped peak with a narrow FWHM of 38 nm, similar to the PL spectrum of the QDs at a slightly longer wavelength (around 4–5 nm). This is attributed to the Förster resonant energy transfer (FRET) from smaller to larger dots within the QDs [31]. Additionally, the inset in Figure 5(c) shows an EL photographic image of a QLED fabricated using our CdSe@ZnS QDs. The bright green emission from this QLED is due to the excellent current injection of the CdSe@ZnS QDs which emit brilliantly.



(a)



(b)



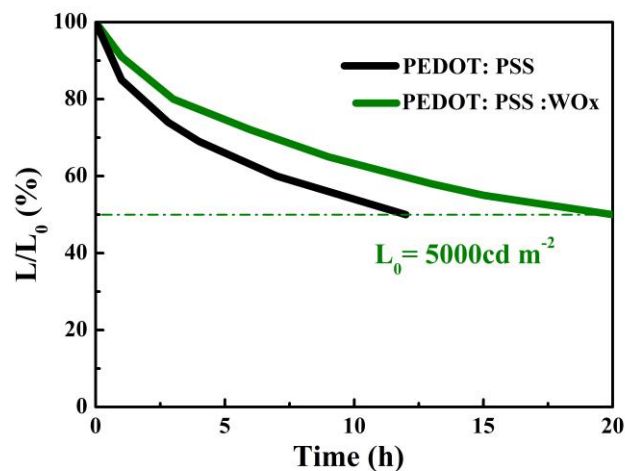
(c)

Figure 5. (a) Current density–luminance–voltage (J–L–V); (b) current efficiency–power efficiency with luminance characteristics for the different volume ratios PEDOT:PSS:WO_x-based QLED; (c) EL spectra of the standard and optimal device, the inset shows the photographic image of the green QLED.

Table 1. The performance parameters of the standard and optimal QLEDs.

Device	$V_T(V)$	$L_{max} (cd\ m^{-2})$	$\eta_P (lm\ W^{-1})$	$\eta_A (cd\ A^{-1})$	FWHM (nm)
Control	2.7	46000	6.5	9.8	38
10:1	2.6	62000	8.9	13.1	38

Compared to PEDOT:PSS HIL, the most significant advantage of using a PEDOT: PSS: WOx film is the significant improvement in the operating lifetime of the device. The stability of a PEDOT:PSS:WOx-based QLED and a PEDOT:PSS-based device were compared, and tests were conducted in air with a simple UV curing epoxy resin encapsulation, as shown in Figure 6. The PEDOT:PSS:WOx-based QLED demonstrated a half-life time of approximately 20 hours when tested under an initial luminance of $5000\ cd\ m^{-2}$. This corresponds to a long device lifetime of approximately 7071 hours at an initial luminance of $100\ cd\ m^{-2}$ ($L_0^n T_{50} = \text{constant}$, $n = 1.5$, which represents the acceleration factor) [10]. This indicates an almost two-fold increase in the operating lifetime compared to the PEDOT:PSS-based QLED, which displayed an operating lifetime of only 12 hours. The enhanced stability of the device can be primarily attributed to the superior thermal stability of inorganic hole transport materials in comparison to their organic counterparts. Furthermore, the device based on PEDOT:PSS: WOx exhibits a higher efficiency and carrier recombination rate when subjected to a luminance of $3000\ cd\ m^{-2}$, which ultimately translates to reduced damage from accumulated carriers.

**Figure 6.** The operating lifetime characteristics of the PEDOT:PSS:WOx-based and PEDOT:PSS-based QLEDs.

3.3. Effect of PEDOT:PSS: WOx on QLED performance

It is commonly accepted that the morphology of the HIL (or HTL) plays a crucial role in the performance of the all-solution-processed QLED, and a smooth surface can effectively reduce the occurrence of micro electrical shorts [18]. Therefore, surface morphology measurements were conducted using both scanning force microscopy (SEM) and atomic force microscopy (AFM). As shown in Figure 7(a-c), the SEM images illustrate the surface morphology of the ITO glass, ITO/PEDOT:PSS, and ITO/PEDOT: PSS: WOx (10:1) respectively. It is apparent that ITO/PEDOT:PSS has a well-formed film that exhibits some clefs, as shown in Figure 7(b). However, the use of a PEDOT:PSS:WOx layer as the anode buffer layer leads to a better surface morphology compared to ITO/ PEDOT:PSS, exhibiting smaller clefs. This indicates that the deposition of the PEDOT: PSS: WOx layer alters the surface morphology of the anode. Figure 6(d-f) displays tapping mode AFM images at the $2\ \mu m \times 2\ \mu m$ scan size of the samples. Figure 7(d) shows that the root

mean square (RMS) roughness of the ITO surface is 2.2 nm. After the PEDOT: PSS: WO_x layer is added, the RMS roughness reduced to 1.02 nm, and the surface becomes much flatter, which is comparable to the PEDOT:PSS modified ITO substrate (with an RMS roughness of 1.25 nm, shown in figure 7(e)). This modification of the surface roughness by WO_x results in low Ohmic contact resistance, serving as a strong foundation for constructing QLED with highly smooth and clear HTL and QDs layers.

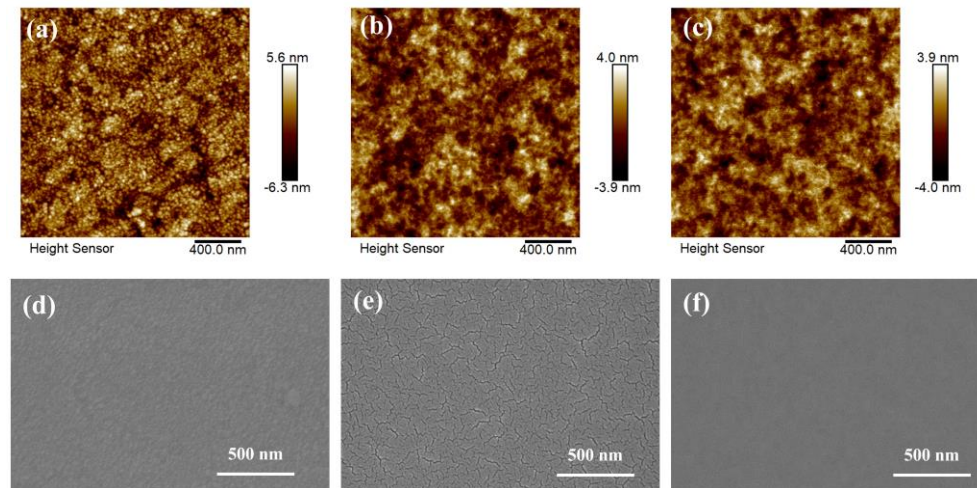


Figure 7. SEM images of (a) the ITO glass, (b) ITO/PEDOT: PSS, (c) ITO/PEDOT: PSS: WO_x (10:1) films; AFM images of (d) the ITO glass, (e) ITO/PEDOT: PSS, (f) ITO/PEDOT: PSS: WO_x (10:1) films.

On the other hand, in order to produce high-quality QLEDs, a high level of transparency in the HIL is required. To assess this, we also measured the transmittance of ITO/PEDOT:PSS and ITO/PEDOT:PSS:PSS:WO_x substrates. The results, as depicted in Figure 8, indicate that all substrates exhibit similar levels of transmittance across the visible spectrum, with consistently high levels (~90%). In the UV region, however, the ITO/PEDOT:PSS:PSS:WO_x substrate showed a slight reduction in light transmittance, attributed to the bandgap transitions of the WO_x film.

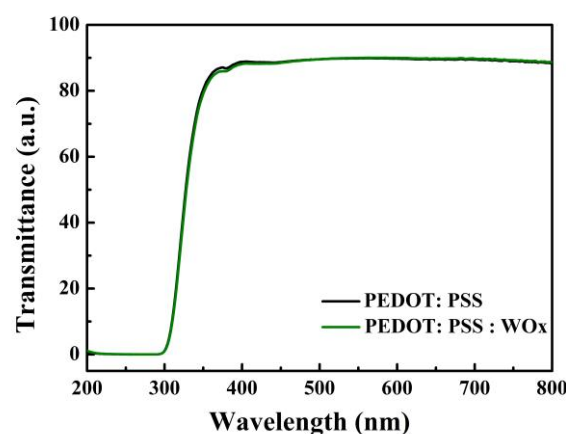


Figure 8. Transmittance of the PEDOT:PSS/glass and PEDOT:PSS: WO_x/glass.

To investigate the hole injection and transport capability of QLEDs with both PEDOT: PSS and PEDOT:PSS:WO_x structures, the Au/HTL/HIL/ITO hole-only devices were analyzed. In this device structure, the large injection barrier at TFB/Au should obstruct electron injection from the Au electrode to TFB. As a result, measuring the J-V characteristic curves can effectively characterize the hole injection and transport capability.

ity. Figure 9 displays the J-V characteristic curves of TFB/PEDOT:PSS and TFB/ PEDOT: PSS: WO_x hole-only devices with Au and ITO electrodes at both ends. The J-V curves of hole-only devices exhibited comparable electrical characteristics to those of QLEDs. Furthermore, hole-only devices containing TFB/PEDOT:PSS:WO_x demonstrated increased current density at high voltages. This finding suggests that incorporating PEDOT: PSS: WO_x enhances the conductivity of holes in QLEDs at elevated voltages, improving their electrical and electro-luminescent performance.

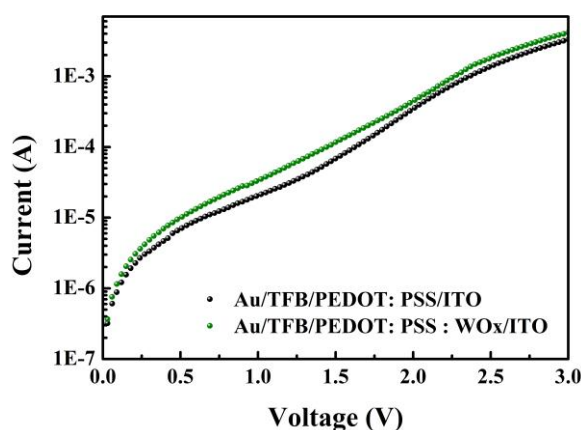


Figure 9. Current density–voltage characteristics of the hole-only devices with pure PEDOT:PSS and PEDOT: PSS: WO_x (10:1) HIL.

4. Conclusions

The findings of this study suggest that using WO_x doped PEDOT:PSS as a hole injection layer can significantly enhance the stability and performance of QLEDs. The QLEDs demonstrated an impressive improvement of approximately 36.9%, which can be attributed to the enhanced hole injection/transmission performance and better Ohmic response of the PEDOT:PSS: WO_x mixture with a volume ratio of 10:1, compared to the pure PEDOT:PSS. The use of stable WO_x instead of problematic PEDOT:PSS resulted in a significant improvement in the stability of the devices. This approach offers a simple, cost-effective, and versatile method to enhance the efficiency and stability of QLEDs.

Author Contributions: Chen, L. and Li, D.; writing—original draft and writing—review and editing; Shang, J. and Jiang, D.; methodology, Du, W. and Liu, S.; formal analysis. All authors have read and agreed to the published version of the manuscript.

Funding: This research was funded by the National Natural Science Foundation of China, grant number 52202168, the Program for Science & Technology Innovation Talents in Universities of Henan Province, grant number 21HASTIT014, the Excellent Youth Fund of Henan Natural Science Foundation, grant number 212300410031, the Natural Science Foundation of Henan Province, China, grant number 202300410098, the Scientific Research Foundation of the Higher Education Institutions of Henan Province, China, grant number 21B140002、23A140019、22B430009, and the Henan University of Engineering Foundation, China, grant number DKJ2019012.

Data Availability Statement: Not applicable.

Conflicts of Interest: The authors declare no conflict of interest.

References

1. Qian, L.; Zheng, Y.; Xue, J.; Holloway, P.H. Stable and efficient quantum-dot light-emitting diodes based on solution-processed multilayer structures. *Nat. Photonics* **2011**, *5*, 543-548.
2. Lim, J.; Bae, W.K.; Kwak, J.; Lee, S.; Lee, C.; Char, K. Perspective on synthesis device structures and printing processes for quantum dot displays. *Opt. Mater. Express* **2012**, *2*, 594-628.
3. Shirasaki, Y.; Supran, G.J.; Bawendi, M.G.; Bulović, V. Emergence of colloidal quantum-dot light-emitting technologies. *Nat. Photonics* **2013**, *7*, 13-23.
4. Dai, X.; Zhang, Z.; Jin, Y.; Niu, Y.; Cao, H.; Liang, X.; Chen, L.; Wang, J.; Peng, X. Solution-processed, high-performance light-emitting diodes based on quantum dots. *Nature* **2014**, *515*, 96-99.
5. Shen, H.; Gao, Q.; Zhang, Y.; Lin, Y.; Lin, Q.; Li, Z.; Chen, L.; Zeng, Z.; Li, X.; Jia, Y.; Wang, S.; Du, Z.; Li, L.S.; Zhang, Z. Visible quantum dot light-emitting diodes with simultaneous high brightness and efficiency. *Nat. Photonics* **2019**, *13*, 192-197.
6. Colvin, V.L.; Schlamp, M.C.; Alivisatos, A.P. Light-emitting diodes made from cadmium selenide nanocrystals and a semiconducting polymer. *Nature* **1994**, *370*, 354-357.
7. Pal, B.N.; Ghosh, Y.; Brovelli, S.; Laocharoensuk, R.; Klimov, V.I.; Hollingsworth, J.A.; Htoon, H. 'Giant' CdSe/CdS core/shell nanocrystal quantum dots as efficient electroluminescent materials: strong influence of shell thickness on light-emitting diode performance. *Nano Lett.* **2012**, *12*, 331-336.
8. Jang, E.; Jang, H. Review: Quantum Dot Light-Emitting Diodes. *Chem. Rev.* **2023**, *123*, 4663-4692
9. Song, J.; Wang, O.; Shen, H.; Lin, Q.; Li, Z.; Wang, L.; Zhang, X.; Li, L.S. Quantum dot LEDs: Over 30% external quantum efficiency light-emitting diodes by engineering quantum dot-assisted energy level match for hole transport layer. *Adv. Funct. Mater.* **2019**, *29*, 1970226.
10. Jong, M.P.D.; Ijzendoorn, L.J.V.; Voigt, M.J.A.D. Stability of the interface between indium-tin-oxide and poly(3,4-ethylenedioxythiophene)/poly(styrenesulfonate) in polymer light-emitting diodes. *Appl. Phys. Lett.* **2000**, *77*, 2255-2257.
11. Kawano, K.; Pacios, R.; Poplavskyy, D.; Nelson, J.; Bradley, D.D.; Durrant, J.R. Degradation of organic solar cells due to air exposure. *Sol. Energy Mater. Sol. Cells* **2006**, *90*, 3520-3530.
12. Yang, X.; Mutlugun, E.; Zhao, Y.; Gao, Y.; Leck, K.S.; Ma, Y.; Ke, L.; Tan, S.T.; Demir, H.V.; Sun, X.W. Light-emitting diodes: solution processed tungsten oxide interfacial layer for efficient hole-injection in quantum dot light-emitting diodes. *Small* **2014**, *10*, 247-252.
13. Lee, S.M.; Shin, D.; Cho, N.K.; Yi, Y.; Kang, S.J. A solution-processable inorganic hole injection layer that improves the performance of quantum-dot light-emitting diodes. *Curr. Appl. Phys.* **2017**, *17*, 442-447.
14. Zhang, Y.; Wang, S.; Chen, L.; Fang, Y.; Shen, H.; Du, Z. Solution-processed quantum dot light-emitting diodes based on NiO nanocrystals hole injection layer. *Org. Electron.* **2017**, *44*, 189-197.
15. Zeng, Q.; Xu, Z.; Zheng, C.; Liu, Y.; Chen, W.; Guo, T.; Li, F.; Xiang, C.; Yang, Y.; Cao, W.; Xie, X.; Yan, X.; Qian, L.; Holloway, P.H. Improving charge injection via a blade-coating molybdenum oxide layer: toward high-performance large-area quantum-dot light-emitting diodes. *ACS Appl. Mater. Interfaces* **2018**, *10*, 8258-8264.
16. Chen, D.; Li, Y.; Dai, X.; Du, H.; Lin, J.; Jin, Y. Synthesis of highly monodisperse Cu₂O nanocrystals and their applications as hole-transporting layers in solution-processed light-emitting diodes. *Chem. Eur. J.* **2019**, *25*, 14767-14770.
17. Kim, W.; Kim, J.K.; Lim, Y.; Park, I.; Choi, Y.S.; Park, J.H. Tungsten oxide/PEDOT: PSS hybrid cascade hole extraction layer for polymer solar cells with enhanced long-term stability and power conversion efficiency. *Sol. Energy Mater. Sol. Cells* **2014**, *122*, 24-30.
18. Chen, L.; Wang, S.; Li, D.; Fan, Y.; Shen, H.; Li, L.S.; Du, Z. Simultaneous improvement of efficiency and lifetime of quantum dot light-emitting diodes with a bilayer hole injection layer consisting of PEDOT: PSS and solution-processed WO₃. *ACS Appl. Mater. Interfaces* **2018**, *10*, 24232-24241.
19. Choi, H.; Kim, B.; Ko, M.J.; Lee, D.K.; Kim, H.; Kim, S.H.; Kim, K. Solution processed WO₃ layer for the replacement of PEDOT: PSS layer in organic photovoltaic cells. *Org. Electron.* **2012**, *13*, 959-968.
20. Zhu, L.Z.; Richardson, B.J.; Yu, Q.M. Inverted hybrid CdSe-polymer solar cells adopting PEDOT: PSS/MoO₃ as dual hole transport layers. *Phys. Chem. Chem. Phys.* **2016**, *18*, 3463-3471.

21. Zhuo, M.P.; Liang, F.; Shi, Y.L.; Hu, Yun.; Wang, R.B.; Chen, W.F.; Wang, X.D.; Liao, L.S. WO₃ nanobelt doped PEDOT: PSS layers for efficient hole-injection in quantum dot light-emitting diodes. *J. Mater. Chem. C* **2017**, *5*, 12343-12348.
22. Lee, M.H.; Chen, L.; Li, X. N.; Zhu, F. MoO₃-induced oxidation doping of PEDOT: PSS for high performance full-solution-processed inverted quantum-dot light emitting diodes. *J. Mater. Chem. C* **2017**, *13*, 10555-10561.
23. Shin, J.S.; Kim, T.Y.; Heo, S.B.; Hong, J.A.; Park, Y.; Kang, S.J. Improving the performance of quantum-dot light emitting diodes via an organic-inorganic hybrid hole injection layer. *RSC Adv.* **2021**, *11*, 4168-4172.
24. Ma, Z.; Tang, L.; Lyu, B. Highly efficient full color light-emitting diodes based on quantum dots surface passivation engineering. *Org. Electron.* **2019**, *70*, 140-148.
25. Youn, J.H.; Baek, S.J.; Kim, H.P.; Nam, D.H.; Lee, Y.; Lee, J. G.; Jang, J. Improving the lifetime of a polymer light-emitting diode by introducing solution processed tungsten oxide. *J. Mater. Chem. C* **2013**, *1*, 3250-3254.
26. Jiménez-González, A.E.; Urueta, J.A.S.; Suárez-Parra, R. Optical and electrical characteristics of aluminum-doped ZnO thin films prepared by solgel technique. *Cryst. Growth* **1998**, *192*, 430-438.
27. Min, J.S.; Kim, S.; Kwon, S.; Kim, J.W. Interface electronic structures of organic light-emitting diodes with WO₃ interlayer: A study by photoelectron spectroscopy. *Org. Electron.* **2009**, *10*, 637-642.
28. Vasilopoulou, M.; Palilis, L.C.; Georgiadou, D.G.; Douvas, A.M.; Argitis, P.; Kennou, S.; Davazoglou, D. Reduction of tungsten oxide: A path towards dual functionality utilization for efficient anode and cathode interfacial layers in organic light-emitting diodes. *Adv. Funct. Mater.* **2011**, *21*, 1489-1497.
29. He, S.; Li, S.; Wang, F.; Wang, A.Y.; Lin, J.; Tan, Z. Efficient quantum dot light-emitting diodes with solution-processable molybdenum oxide as the anode buffer layer. *Nanotechnology* **2013**, *24*, 175201.
30. Zhang, T.; Liu, P.; Zhao, F.; Tan, Y.; Sun, J.; Xiao, X.; Wang, Z.; Wang, Q.; Zheng, F.; Sun, X.W.; Wu, D.; Xing, G.; Wang, K. Electric dipole modulation for boosting carrier recombination in green InP QLEDs under strong electron injection. *Nanoscale Adv.* **2023**, *5*, 385.
31. Lin, Q.; Shen, H.; Wang, H.; Wang, A.; Niu, J.; Qian, L.; Guo, F.; Li, Li.S. Cadmium-free quantum dots based violet light-emitting diodes: High-efficiency and brightness via optimization of organic hole transport layers. *Org. Electron.* **2015**, *25*, 178-183.